Journal of Zhejiang University-SCIENCE A (Applied Physics & Engineering)
ISSN 1673-565X (Print); ISSN 1862-1775 (Online)
www.jzus.zju.edu.cn; www.springerlink.com
E-mail: jzus@zju.edu.cn

Catenary insulator defect detection based on contour features and gray similarity matching*

Ping TAN[1], Xu-feng LI[1], Jin-mei XU[1], Ji-en MA[†‡2], Fei-jie WANG[3], Jin DING[1], You-tong FANG[2], Yong NING[1]

[1]*School of Automation and Electrical Engineering, Zhejiang University of Science and Technology, Hangzhou 310023, China*

[2]*College of Electrical Engineering, Zhejiang University, Hangzhou 310027, China*

[3]*UniTTEC Co., Ltd., Hangzhou 310051, China*

[†]E-mail: majien@zju.edu.cn

Received July 18, 2019; Revision accepted Oct. 9, 2019; Crosschecked Dec. 12, 2019

Abstract: Insulators are the key components of high speed railway catenaries. Insulator failures can cause outages and affect the safe operation of high speed railways. It is important to perform insulator defect detection. Due to the collection of insulator images by moving catenary inspection vehicles, the consistency of the images is poor, and the number of insulator defect samples is very small. An algorithm of deep learning and conventional template matching cannot meet the requirements of insulator defect detection. This paper proposes a fusion algorithm based on the shed contour features and gray similarity matching. High accuracy and consistency of contour extraction and precise separation of each insulator shed were realized. An insulator defect detection model based on the spacing distance of the sheds and the gray similarity was constructed. Experiments show that the method based on the contour features and gray similarity matching can effectively classify normal insulators and defective insulators. Recall of 99.50% and high precision of 91.71% were achieved in the test of the image data set, and this can meet the requirements for the reliability and high precision of a detection algorithm for catenary insulators.

Key words: High speed railway insulator; Defect detection; Contour extraction; Shed separation; Gray similarity
https://doi.org/10.1631/jzus.A1900341 **CLC number:** TM216; TP311

1 Introduction

China has the world's largest high speed railway network with the most advanced technology (Chen et al., 2014; Tan, 2014; Tan et al., 2016). The catenary is one of the key subsystems of the high speed railway which includes the support device, suspend device, post, and base. In order to ensure the safety and reliability of the system, China Railway Corporation has released the "General Technical Specification for the High Speed Railway Power Supply Safety Detection and Monitoring System (6C System)" (Wan, 2013) which contains six sets of subsystem from C1 to C6, and C4 is one of the most important subsystems. The insulator is an important component of the catenary support device, and plays the roles of support, insulation, and isolation. Insulator failure may result in catenary outages and affect the safe operation of the high speed trains. Thus, it is very important to detect insulator defects. There are two main methods to detect defects, both of which rely substantially on railway maintenance crews.

The number of catenary insulators is huge, the efficiency of manual inspection is low, and there is the

‡ Corresponding author

* Project supported by the National Natural Science Foundation of China (Nos. 51677171, 51637009, 51577166, and 51827810), the Zhejiang Provincial Natural Science Foundation of China (No. LY17C100001), the National Key R&D Program of China (No. 2018YFB0606000), and the China Scholarship Council (No. 201708330502)

ORCID: Ping TAN, https://orcid.org/0000-0001-8656-3514

possibility of false and missed detection. Thus, it is of great significance to develop a intelligent catenary insulator defect detection system.

The main research carried out so far includes: Zhang and Liu (2014) used the Harris corner and spectral clustering method to achieve anti-rotation matching and damage/inclusion foreign body fault detection of insulators; Guo et al. (2015) used the method of corner registration and image difference to realize the fault detection of insulators; Ai and Jin (2016) used ultraviolet imaging technology combined with image processing technology to determine insulator contamination status; Dang et al. (2019) detected the contamination status anomaly of railway insulators based on possibilistic C-means (PCM) and texture features; Yao et al. (2018) carried out insulator identification and contamination detection based on the speed up robust features (SURF) sample library and hue, saturation, value (HSV) color range; Yang et al. (2019) used the Sobel improved algorithm to recognize crack insulator sheds; Yang et al. (2018) detected the surface wetting characteristics of the pollution insulator based on phase angle difference; Wu et al. (2019) proposed an improved lightweight network based on the YOLOv3 detection architecture, which realized the positioning and defect detection of the insulator. Despite this research, there remain some problems. For example, the reliability or accuracy of the detection algorithm cannot meet the requirement for a C4 subsystem.

The catenary inspection vehicle installed with the C4 subsystem runs at a speed of 160 km/h, and takes the catenary image during train movement. The image of the catenary support device is shown in Fig. 1.

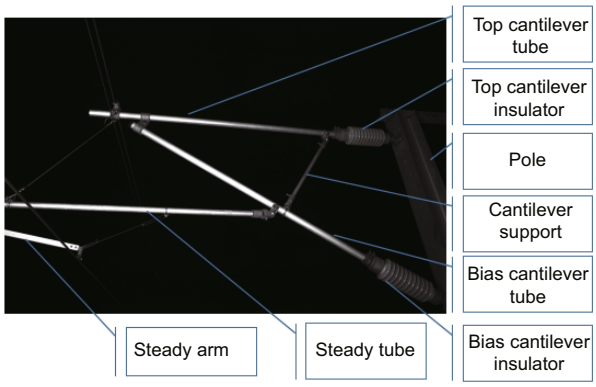

Fig. 1 Structure image of the high speed railway catenary support device

There are many kinds of catenary components, and different components need to be detected by different methods. This article mainly focuses on the study of the insulator defect intelligent detection algorithms and technologies according to the C4 image characteristics.

2 Overall algorithm model

As shown in Fig. 1, there are different support components in the image, including top cantilever insulators and bias cantilever insulators. In order to achieve accurate judgment of insulator defects, the insulator target region should be identified. Deep learning (Zhang and Zhu, 2018) algorithms are applied to insulator recognition, positioning, and interception. Based on the output of the deep learning algorithm, the insulator defect detection can be implemented.

Insulator defects mainly include the breakage, dirt, foreign body, and flashover. The number of samples of insulator defects is very limited, and the defect characteristics are unpredictable. The deep learning algorithm cannot meet the requirements of insulator defect detection. In addition, since the images are taken while the inspection vehicle is moving, the shooting angle and exposure factors are different for each image, and the consistency of the images of different insulators is very poor. Taking images for defect detection should be avoided as much as possible in the extreme weather conditions, because rain or snow may cause dirt or foreign body or other defects. Even with the same insulator, the images taken at different times are also very different, so the general template matching algorithm also cannot meet the requirements.

For different insulator sheds on the same insulator image, the impacts of shooting angle and exposure factor are the same. By extracting and analyzing the characteristics of different insulator sheds of the same insulator, insulator defects can be detected. This paper proposes a defect detection method based on the contour features and gray similarity of sheds on the same insulator. The overall algorithm model is shown in Fig. 2, and is mainly composed of two parts.

The first part is the algorithms for the insulator feature extraction and gray pixel restoring inside the shed contour. Based on the image output of the

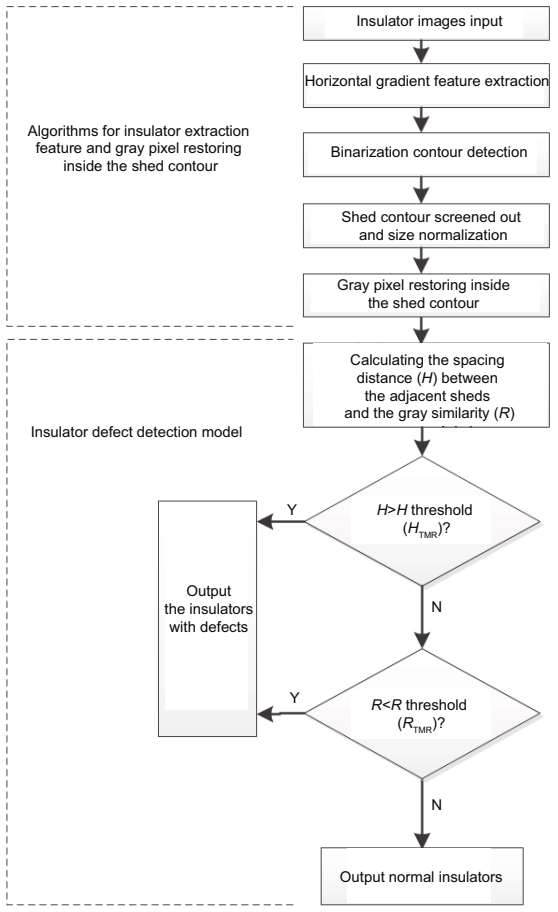

Fig. 2 Overall model of insulator defect detection

deep learning algorithm, research is needed for the horizontal gradient feature extraction of the insulator images and the shed contour detection. Then fine tuning and unifying of the shed contour size algorithm is studied, followed by the gray restoration inside the shed contours.

The second part is the insulator defect detection model. Based on the shed spacing distance and gray similarity calculation, the detection model of the insulator defects is constructed and the criteria of the defects are studied. Then the insulator defects can be detected, and the normal insulator and defective insulator can be classified and output.

Intelligent detection of catenary insulator defects is based on image processing technology, so the establishment of a catenary insulator image data set is the primary task. In this research, a data set was created with the actual catenary rod insulator images. Of the total of 600 insulator images, 400 are normal insulators and 200 are defective insulators, as shown in Fig. 3.

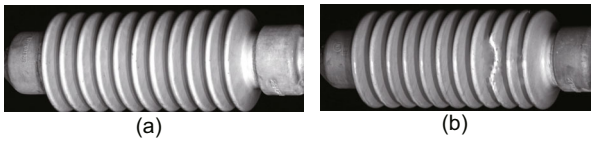

Fig. 3 Original images of the insulator with normal insulator (a) and defective insulator (b)

3 Insulator feature extraction and pixel restoration algorithm of sheds

Based on the above analysis, it is known that defect detection by the comparison of the sheds on the same insulator is a reasonable technical route. The characteristics of the insulator and the extraction of the contour features of the insulator are studied first, and then it is necessary to carry out the research on precise positioning and gray feature restoration of the insulator sheds. This will provide reliable data input for insulator defect detection.

3.1 Gradient feature extraction

By analyzing the insulator image characteristics, it can be found that the shed positioning can be determined by edge detection. The commonly used edge detection algorithms include Canny edge detection, Laplace edge detection, and Sobel edge detection (Haralick, 1984; Canny, 1986; Ziou and Tabbone, 1998; Pellegrino et al., 2004; Wu et al., 2007).

The experimental result in Section 5.1 shows that the shed edge cannot be detected correctly by a single edge detection algorithm, and the insulator shed contour cannot be accurately extracted.

The characteristics of the insulator images should be analyzed in detail. Then the effective detection method for the insulator shed contour can be designed, based on the insulator characteristic analysis result and the Sobel operator and binarization edge detection. The first step is to extract the gradient features of the insulator.

The so-called edge is actually a collection of points with great changes in gray on the image. When the insulator is viewed in the horizontal direction, the gray level difference between adjacent sheds is large. That is, the gradient features in the horizontal direction are more obvious than the other

direction. Then, according to the principle of the Sobel algorithm, the following 3×3 convolution kernel is designed:

$$\begin{bmatrix} -1 & 0 & 1 \\ -2 & 0 & 2 \\ -1 & 0 & 1 \end{bmatrix}, \tag{1}$$

and the insulator image is convoluted to obtain the gradient features in the horizontal direction, as shown in Fig. 4.

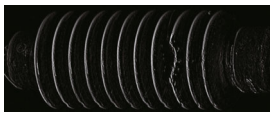

Fig. 4 Horizontal gradient feature extraction results of insulator

3.2 Contour extraction of insulator sheds

The horizontal gradient features of the insulator effectively outline the contour features of each shed. The next step is to extract the contour information of each shed, that is, the pixel point information and coordinate information of each shed contour. Firstly, the horizontal gradient feature map of the insulator is converted into a binary image. The binarization formula is

$$s = T(r) = \begin{cases} 255, & A \le r \le B, \\ 0, & \text{otherwise}, \end{cases} \tag{2}$$

where r is the gray value of the pixel of the original image, A and B are the thresholds of the gray value, and s is the gray value of the pixel after binarization. The binarized image is as shown in Fig. 5.

Fig. 5 Binarization of horizontal gradient features

Secondly, using the contour tracking algorithm (Suzuki and be, 1985), the contour information is extracted. The main purpose is to find the region where the gray value of the image has changed, and establish the binary image topology to obtain the contour information. Since we only need the contour information of each shed of the insulator, and all the contour information obtained by the above method contains the contour information of each shed and the non-contour information of the shed, it is necessary to filter the contour information based on the contour size and the length to width ratio of the contour. After screening out, the contour information of each insulator shed is finally obtained.

Finally, the comparison of the gray similarity of the shed is adopted, and this requires high positioning precision of the pixel points of the sheds, so it is necessary to fine-tune the scale of the sheds, that is, to unify the contour size of the sheds.

3.3 Pixel restoration of insulator sheds

The gray similarity comparison in each insulator shed is an effective method for insulator defect detection. However, the contour information extraction for each insulator and the pixel restoration of each insulator shed obtained above need to be performed. Pixel restoration is to fill the point inside the shed contour with the pixel value corresponding to the position on the original image. In order to determine the search region of the shed pixel restored on the original image, the coordinate information of the upper left corner vertex and lower right corner vertex is obtained according to the shed contour information. The formulas are given by

$$P_{\mathrm{lt}}(x, y) = \min(\mathrm{ctrs}(x, y)), \tag{3}$$

$$P_{\mathrm{rb}}(x, y) = \max(\mathrm{ctrs}(x, y)), \tag{4}$$

where P_{lt} is the coordinate information of the upper left corner of the shed contour, P_{rb} is the coordinate information of the lower right corner of the shed contour, and ctrs is the coordinate information set of each pixel point of the shed contour.

Based on the above two vertices, the search region of the contour pixel restoration is determined on the insulator original image. The adopted search mode is to search pixel points firstly in the horizontal direction, and the coordinates of all the pixel points in the region are traversed once, and it is determined whether the coordinates of the pixel points are within the coordinate region surrounded by the shed contour. If so, the corresponding position in the shed contour is filled with pixel gray value, otherwise, not filled. The formula is shown as

$$G_{P(x,y)} = \begin{cases} G'_{P(x,y)}, & P(x, y) \in \sigma_{\mathrm{ctrs}}, \\ 0, & P(x, y) \notin \sigma_{\mathrm{ctrs}}, \end{cases} \tag{5}$$

where P is the pixel point coordinates, G is the point gray value to be filled in the shed contour, G' is the

point gray value on the original image, and σ_{ctrs} is the shed contour region.

The above is a pixel restoration process inside the insulator shed contour. The insulator shed contour is also restored by the above method, and the insulator shed can be obtained. The results are shown in Fig. 6.

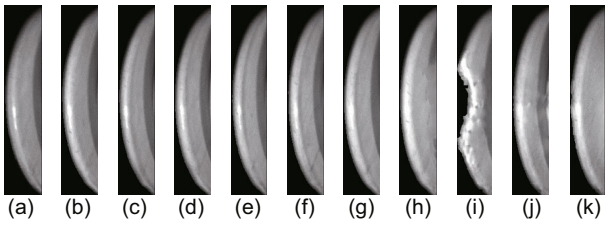

Fig. 6 Pixel restoration results in the contour of each insulator shed (a)–(k)

In Fig. 6, the obtained insulator sheds from left to right correspond to the sheds on the original image of the insulator. Compared with the original image, the information of the insulator sheds extracted according to the method is accurate and effective, and each insulator shed precise separation is determined, which provides favorable data support for subsequent insulator defect detection.

4 Insulator defect detection model

Based on the information of the insulator shed contour and gray, together with the precise insulator shed separation, the insulator defect detection model was established. When the insulator shed broken area is too large, the contour information of the shed may not be effectively extracted, which will affect the result of the final defect detection. Therefore, when we carry out insulator defect detection, we should calculate the spacing distance between each insulator shed first, and then we implement the shed similarity comparison.

4.1 Spacing distance calculation of insulator sheds

Two vertices of the shed contour are obtained by Eqs. (3) and (4), then the coordinates of the center point of the contour are calculated. The spacing distance of each insulator shed is calculated by Eq. (6).

H is the spacing distance between adjacent sheds of the insulator. After the spacing distance of each shed is calculated, and the spacing distance threshold is set, the shed defect can be detected by comparing with the spacing distance threshold.

4.2 Similarity detection algorithm of insulator sheds

Image similarity comparison, that is, image matching algorithm, is mainly divided into three categories: gray-based matching, feature-based matching, and relationship-based matching algorithms. The gray-based matching algorithm is directly based on the gray value of the pixel, so it can meet the requirement of the high speed railway catenary insulator defect detection for high reliability and accuracy. Therefore, the gray-based matching algorithm is selected in this study.

Based on the gray matching algorithm, the gray value of the image pixel is used for calculating the similarity of the image, and the core is the selection of the similarity measure function. Since Rosenfeld and Kak (1982) proposed the normalized cross correlation (NCC) algorithm, it has become a widely used image matching algorithm with high precision and strong anti-interference ability. It is not affected by linear transformation of gray values. The calculation formula of the NCC algorithm (Rosenfeld and Kak, 1982; Briechle and Hanebeck, 2001) is shown in Eq. (7), where $R(i,j)$ is the matching result of the image to be matched at the position of the point (i,j). The closer the value of R is to 1, the higher the similarity is. I^{ij} is the subimage at the point (i,j), I_{xy} is the gray value of the subimage to be matched at the point (x,y), T_{xy} is the gray value of the template image at the point (x,y), $\bar{I}^{ij}$ is the average gray value of the subimage, $\bar{T}$ is the average gray value of the template image, w is the template image width, and h is the template image height.

Since the image to be matched and the template image in this paper are both individual shed images of the insulator, that is, the I and T scales are the same size, so we obtain the formula of Eq. (8), where R is the gray similarity matching result of two adjacent insulator sheds, SH1 and SH2 are two adjacent insulator sheds, w is the width of the shed image, and h is the height of the shed image.

According to Eq. (8), the gray similarity R of each two adjacent insulator sheds is sequentially calculated. The R values of the two normal insulator sheds and the R values of the normal shed and the defective shed are analyzed. These will be compared

$$H_i = |\frac{P_{\mathrm{lt}}(x,y)_i + P_{\mathrm{rb}}(x,y)_i}{2} - \frac{P_{\mathrm{lt}}(x,y)_{i+1} + P_{\mathrm{rb}}(x,y)_{i+1}}{2}|, \tag{6}$$

$$R(i,j) = \frac{\sum_{x=1}^{w}\sum_{y=1}^{h}|I_{xy}^{ij} - \bar{I}^{ij}| \times |T_{xy} - \bar{T}|}{\sqrt{\sum_{x=1}^{w}\sum_{y=1}^{h}(I_{xy}^{ij} - \bar{I}^{ij})^2 \times \sum_{x=1}^{w}\sum_{y=1}^{h}(T_{xy} - \bar{T})^2}}, \tag{7}$$

$$R = \frac{\sum_{x=1}^{w}\sum_{y=1}^{h}\mathrm{SH1}_{xy} \times \mathrm{SH2}_{xy} - \frac{1}{w\times h}\sum_{x=1}^{w}\sum_{y=1}^{h}\mathrm{SH1}_{xy} \times \sum_{x=1}^{w}\sum_{y=1}^{h}\mathrm{SH2}_{xy}}{\sqrt{\sum_{x=1}^{w}\sum_{y=1}^{h}\mathrm{SH1}_{xy}^2 - \frac{1}{w\times h}(\sum_{x=1}^{w}\sum_{y=1}^{h}\mathrm{SH1}_{xy})^2} \times \sqrt{\sum_{x=1}^{w}\sum_{y=1}^{h}\mathrm{SH2}_{xy}^2 - \frac{1}{w\times h}(\sum_{x=1}^{w}\sum_{y=1}^{h}\mathrm{SH2}_{xy})^2}}. \tag{8}$$

with the set threshold value, and whether the insulator has defects or not can be determined.

5 Experimental testing and analysis

5.1 Comparison of the insulator shed contour extraction

In order to verify the performance of the insulator contour feature extraction algorithm, the mainstream edge detection algorithms are selected for comparison experiments, which include Canny edge, Laplace edge, Sobel edge, and edge contour detection methods. The results are shown in Fig. 7.

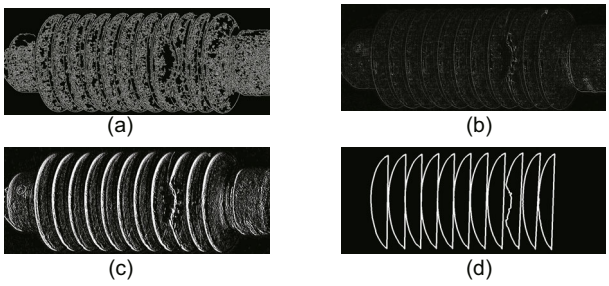

Fig. 7 Comparison tests of insulator shed contour detection with Canny edge detection result (a), Laplace edge detection result (b), Sobel edge detection result (c), and edge contour detection result of this study (d)

From Fig. 7, it can be seen that the Canny algorithm is not sensitive to the insulator shed contour. The extracted edge information has no difference of strong or weak points, and much edge information is detected on one shed. Even if the threshold of the algorithm is adjusted, the interference of invalid edge information cannot be effectively eliminated when extracting the insulator shed contour information.

The Laplace algorithm is sensitive to the edge contour of the shed, but the algorithm has poor anti-interference ability to noise. Some noise edge information is also calculated. As with the Canny algorithm, there are more invalid edge information interferences, which cannot effectively extract the shed contour.

Strong edge information of the shed edge can be obtained by the Sobel algorithm. Compared with the previous two kinds of algorithms, the Sobel algorithm has achieved better detection results. However, it still does not focus the detected information on each insulator shed edge. Sobel edge detection includes horizontal gradient features and vertical gradient features, but the separation of insulator sheds should mainly be based on horizontal gradient features.

Thus, this study proposes the insulator shed edge contour extraction method based on the Sobel algorithm. Although the Sobel algorithm detects the contour features of the edge of the shed, there are still many invalid edge information interferences, and we need to design algorithms to effectively filter the interference information and extract the contour information of the sheds.

This study's edge detection method mainly obtains the shed arc-shaped edge, and arc ends are connected with a straight line. It can be concluded that the contour extraction method of the insulator sheds designed in this study is successful, and the contour information of each insulator shed is accurately and effectively extracted. This provides a basis for the following defect detection.

5.2 Comparison of the insulator shed spacing distance and similarity

Based on the insulator defect detection model, we carried out a test on rod insulators. The test content is mainly divided into two parts. One is the insulator shed spacing distance calculation, and the other is the gray similarity detection of the shed. Both are based on the contour information of the insulator shed. The contour extraction effect of the insulator shed is tested first. The results are as shown in Table 1.

In Table 1, insulator 3 is a broken insulator. The broken area of one shed is too large and the contour of this shed cannot be extracted. It can also be seen that the shed contour of the other three insulators of sheds are extracted accurately, regardless of the presence or absence of defects.

Based on the extracted shed contours, the insulator shed spacing distance calculation and gray similarity detection test are performed, and the results are shown in Figs. 8 and 9.

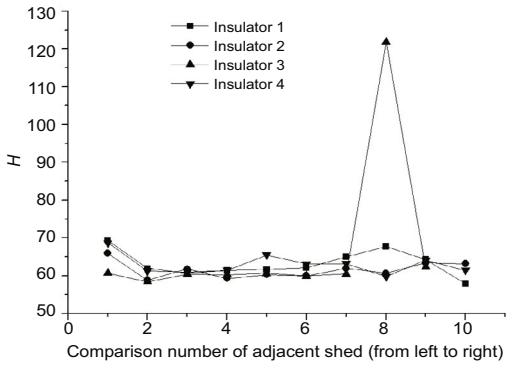

Fig. 8 Calculation result of the insulator shed spacing distances

From the original image of the insulator 1 shown in Table 1, it can be seen that there is a defect in the ninth shed from the left to the right. From the insulator shed contour in Table 1, it can be seen that the contour extraction of each shed is also accurate. Combining the information shown in Figs. 8 and 9, the analysis is shown below.

Insulator 1 is a defective insulator. It can be seen from Fig. 8 that the calculated H value of the shed spacing distance fluctuates around 60, which belongs to the normal range and has no abnormal value, indicating that insulator 1 has no shed missing (including the case that the shed broken area is large). It can be seen from Fig. 9 that the eighth and ninth R values (from left to right) are about 0.75. The closer the R value is to 1, the more similar the two sheds are. The R values of other sheds are all above 0.9. It can be inferred that insulator 1 is a defective insulator and the ninth shed has defects, which is in line with the original image.

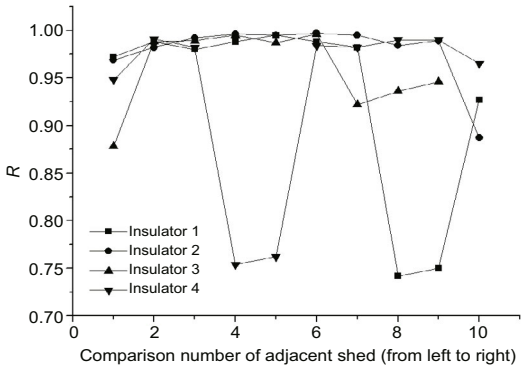

Fig. 9 Gray similarity detection result of the insulator sheds

Insulator 2 is a normal insulator without any defects. From the results of the shed contour, it can be seen that the contour extraction of each shed is also accurate. As can be seen from Fig. 8, the calculated H value of the shed spacing distance fluctuates around 60, which is also in the normal range, and there is no abnormal value, indicating that the insulator 2 has no shed missing defect. As can be seen from Fig. 9, the R values of all the sheds fluctuate around 0.9, and there was no abnormally low value. It can be inferred that insulator 2 has no defects and conforms to the original image.

From the original image of insulator 3 shown in Table 1, the ninth shed (from left to right) has defects. However, from the result of the shed contours, it can be seen that there is one shed contour which has not been extracted, and the contour extraction of other sheds is accurate. As can be seen from Fig. 8, the eighth H value is abnormal, slightly higher than 120, that is, the spacing distance between the eighth shed and the ninth shed, and the H values of other sheds are in the normal range. As can be seen from Fig. 9, the R values of the sheds are above 0.85, and there is no abnormally low value. Therefore, it can be inferred that insulator 3 has a missing shed defect, which is in accordance with the original image.

From the original image of insulator 4 in Table 1,

Table 1 Insulator shed contour extraction results

Insulator number	Original insulator	Insulator shed contour
1	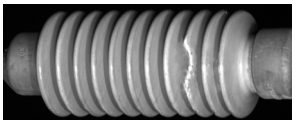	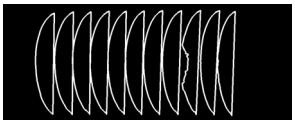
2	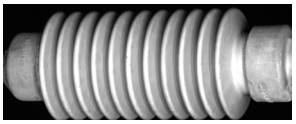	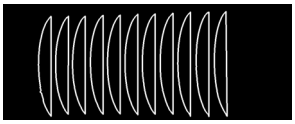
3	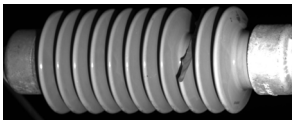	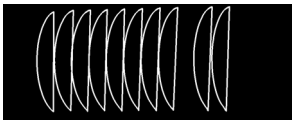
4	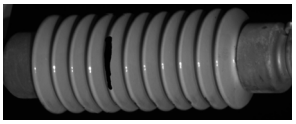	

it can be seen that the fifth shed from the left to the right has defects. From the result of the shed contour, it can be seen that the contour extraction of each shed is also accurate. As can be seen from Fig. 8, the calculated H value of the shed spacing distance is within the normal range, indicating that insulator 4 has no shed missing defect. As can be seen from Fig. 9, the fourth and fifth R values are around 0.75, slightly lower than the others. The R values of the other sheds are about 0.95. According to the R value, it can be inferred that the fifth shed of the insulator 4 has defects, which is in accordance with the original image.

5.3 Evaluation of the insulator defect detection model

According to the analysis, we can confirm that when there is a shed missing defect in the insulator, it can be clearly judged from the shed spacing distance H. Therefore, we set and adjust the threshold of the gray similarity R of the shed, and adjust the range from 0.5 to 0.95. The step size of each adjustment is 0.05. The value exceeding the R threshold range is classified as signifying a defective insulator. The image data set was tested to evaluate the performance of the insulator defect detection model. The evaluation indicators are as follows.

Recall: The ratio of all the defective insulators detected in the image data set that are correctly classified as defective insulators. The calculation formula is

$$\text{Recall} = \frac{\text{TP}}{\text{TP} + \text{FN}}, \tag{9}$$

where TP (true positive) is the number of defective insulators correctly classified as defective; FN (false negative) is the number of defective insulators that are misclassified as normal.

Precision: The ratio of TP in the classification of defective insulators, which is given as

$$\text{Precision} = \frac{\text{TP}}{\text{TP} + \text{FP}}, \tag{10}$$

where FP (false positive) is the number of normal insulators classified as defective.

Miss rate (MR): As opposed to the Recall, the formula is

$$\text{MR} = 1 - \text{Recall}. \tag{11}$$

False rate (FR): The ratio of FP to the total number of normal insulators, which is given as

$$\text{FR} = \frac{\text{FP}}{\text{NS}}, \tag{12}$$

where NS (normal sum) is the total number of normal insulators in the image data set.

According to the above evaluation indicators, the relationship curve between Recall and Precision is drawn. The result is shown in Fig. 10.

It can be seen from Fig. 10 that the insulator defect detection model of this study has better performance. The point where the Recall and the Precision are superior is selected, that is, the threshold

Table 2 Insulator defect detection result

Image item	Total number of insulator images	Number of defect images detected	Number of defect images correctly recognized	Recall (%)	Precision (%)	MR (%)	FR (%)
Insulator	400+200	217	199	99.50	91.71	0.50	4.50

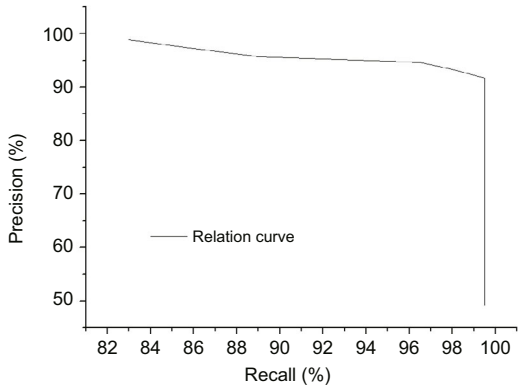

Fig. 10 Relationship curve between Recall and Precision

of R is set to 0.85, and the specific data is shown in Table 2.

It can be seen that the insulator defect detection model designed in this study maintains a high defect detection accuracy, and its false detection rate is also low, within an acceptable range. A defective insulator image incorrectly recognized was analyzed, and it was found that the foreign body just covered the two sheds on the outermost side in a large range, and the contour of the shed was not extracted. For this defect, the calculation of the shed spacing distance can be considered. First, it is judged whether the shed at the beginning and the end of the insulator is extracted; then the normal insulator which is undetected is analyzed. Most of the problems are caused by the fact that the first shed of the insulator is not accurately separated from the connected background, and a part is related to the quality problem of the captured insulator image. The edges of the sheds are relatively vague. For such cases, an edge enhancement algorithm can be designed to make the edges of the extracted sheds clear and smooth.

6 Conclusions

In this paper, based on the structural features of the insulator, a detection model based on the contour and gray similarity of the shed is proposed. By accurately extracting the insulator shed contour features, the model separates the insulator sheds, and adopts the method of calculating the spacing distance and gray similarity of each shed. This can achieve the accurate detection of insulator defects with high reliability even when the insulator image consistency is poor. It provides a reliable and accurate solution for defect detection of high speed railway catenary insulators.

Contributors

Ping TAN and Xu-feng LI designed the research. Ping TAN, Xu-feng LI, Ji-en MA, and Jin DING processed the corresponding data. Ping TAN and Xu-feng LI wrote the first draft of the manuscript. Jin-mei XU, Ji-en MA, Fei-jie WANG, Jin DING, You-tong FANG, and Yong NING helped to organize the manuscript. Ping TAN, Xu-feng LI, and Jin-mei XU revised and edited the final version.

Conflict of interest

Ping TAN, Xu-feng LI, Jin-mei XU, Ji-en MA, Fei-jie WANG, Jin DING, You-tong FANG, and Yong NING declare that they have no conflict of interest.

References

Ai JY, Jin LJ, 2016. Rod porcelain insulator filth state detection of catenary based on ultraviolet image. *Transactions of China Electrotechnical Society*, 31(10):112-118 (in Chinese). https://doi.org/10.3969/j.issn.1000-6753.2016.10.013

Briechle K, Hanebeck U, 2001. Template matching using fast normalized cross correlation. Proceedings of the SPIE 4387, Optical Pattern Recognition XII, p.95-102. https://doi.org/10.1117/12.421129

Canny J, 1986. A computational approach to edge detection. *IEEE Transactions on Pattern Analysis and Machine Intelligence*, PAMI-8(6):679-698. https://doi.org/10.1109/TPAMI.1986.4767851

Chen RP, Chen JM, Wang HL, 2014. Recent research on the track-subgrade of high-speed railways. *Journal of Zhejiang University-SCIENCE A (Applied Physics & Engineering)*, 15(12):1034-1038. https://doi.org/10.1631/jzus.A1400342

Dang ST, Ke J, Wu WH, et al., 2019. The contamination status anomaly detection of railway insulator based on

PCM and texture feature. *Insulators and Surge Arresters*, (2):197-201 (in Chinese).
https://doi.org/10.16188/j.isa.1003-8337.2019.02.034

Guo XG, Liu ZG, Zhang GN, et al., 2015. Fault detection of catenary insulator based on corner matching and image differencing. *Proceedings of the CSU-EPSA*, 27(2):8-14 (in Chinese).
https://doi.org/10.3969/j.issn.1003-8930.2015.02.002

Haralick RM, 1984. Digital step edges from zero crossing of second directional derivatives. *IEEE Transactions on Pattern Analysis and Machine Intelligence*, PAMI-6(1):58-68.
https://doi.org/10.1109/TPAMI.1984.4767475

Pellegrino FA, Vanzella W, Torre V, 2004. Edge detection revisited. *IEEE Transactions on Systems, Man, and Cybernetics, Part B (Cybernetics)*, 34(3):1500-1518.
https://doi.org/10.1109/TSMCB.2004.824147

Rosenfeld A, Kak AC, 1982. Digital Picture Processing, 2nd Edition. Academic Press, San Diego, USA.
https://doi.org/10.1016/B978-0-12-597302-1.50007-4

Suzuki S, be K, 1985. Topological structural analysis of digitized binary images by border following. *Computer Vision, Graphics, and Image Processing*, 30(1):32-46.
https://doi.org/10.1016/0734-189X(85)90016-7

Tan P, 2014. Studies on Key Technologies of Safety and Intelligent Control for Intercity Railway On-board Train Control Systems. PhD Thesis, Zhejiang University, Hangzhou, China (in Chinese).

Tan P, Ma JE, Zhou J, et al., 2016. Sustainability development strategy of China's high speed rail. *Journal of Zhejiang University-SCIENCE A (Applied Physics & Engineering)*, 17(12):923-932.
https://doi.org/10.1631/jzus.A1600747

Wan GH, 2013. Unified information platform of traction power supply for the center with 6C system. *Value Engineering*, 32(13):197-198 (in Chinese).
https://doi.org/10.3969/j.issn.1006-4311.2013.13.108

Wu J, Ye XQ, Gu WK, 2007. An adaptive fuzzy filter for coding artifacts removal in video and image. *Journal of Zhejiang University-SCIENCE A*, 8(6):841-848.
https://doi.org/10.1631/jzus.2007.A0841

Wu T, Wang WB, Yu L, et al., 2019. Insulator defect detection method for lightweight YOLOV3. *Computer Engineering*, 45(8):275-280 (in Chinese).
https://doi.org/10.19678/j.issn.1000-3428.0053695

Yang L, Zhang F, Bi JK, et al., 2018. Wetting characteristics and influential factors of pollution deposited on insulators based on phase angle difference. *High Voltage Engineering*, 44(8):2556-2564 (in Chinese).
https://doi.org/10.13336/j.1003-6520.hve.20180731015

Yang QJ, Niu ZY, Feng XY, et al., 2019. Sobel improved algorithm for insulator ceramic crack recognition. *Journal of Heilongjiang University of Science and Technology*, 29(2):190-195 (in Chinese).
https://doi.org/10.3969/j.issn.2095-7262.2019.02.013

Yao XT, Zhang YP, Gao Y, et al., 2018. Research on vision-based technology of contamination detection in overhead line insulators. *Journal of Lanzhou Jiaotong University*, 37(1):65-72 (in Chinese).
https://doi.org/10.3969/j.issn.1001-4373.2018.01.011

Zhang GN, Liu ZG, 2014. Fault detection of catenary insulator damage/foreign material based on corner matching and spectral clustering. *Chinese Journal of Scientific Instrument*, 35(6):1370-1377 (in Chinese).
https://doi.org/10.19650/j.cnki.cjsi.2014.06.023

Zhang QS, Zhu SC, 2018. Visual interpretability for deep learning: a survey. *Frontiers of Information Technology & Electronic Engineering*, 19(1):27-39.
https://doi.org/10.1631/FITEE.1700808

Ziou D, Tabbone S, 1998. Edge detection techniques: an overview. *International Journal of Pattern Recognition and Image Analysis*, 8(4):537-559.

中文概要

题　目：基于轮廓特征及灰度相似度匹配的接触网绝缘子缺陷检测

目　的：在图像缺陷样本少和一致性差的情况下，实现精确可靠的接触网绝缘子缺陷检测。

创新点：提出一种基于瓷片轮廓特征及灰度相似度匹配的融合算法，实现了绝缘子瓷片的轮廓提取及绝缘子各瓷片的精准分离，并构建了基于瓷片间距和灰度相似度匹配的绝缘子缺陷检测模型。

方　法：1. 采用同一个绝缘子相邻瓷片两两比较的方法进行缺陷检测，解决图像缺陷样本少和一致性差的问题。2. 分两步进行检测（Fig. 2）：（1）基于水平梯度特征提取绝缘子各瓷片轮廓，并对瓷片轮廓内像素进行复原；（2）计算瓷片间距和灰度相似度，并与设置的阈值进行比较以区分正常绝缘子和缺陷绝缘子。

结　论：1. 实验表明，基于轮廓特征及灰度相似度匹配的方法能够有效区分正常绝缘子和缺陷绝缘子。2. 在图片数据集中，测试达到了99.50% 的高召回率和91.71%的高精确度，满足了目前较高水平的接触网绝缘子缺陷检测的要求。

关键词：高铁绝缘子；缺陷检测；轮廓提取；瓷片分离；灰度相似度